SSC18-WKI-07

Single GPS Antenna Attitude Vector Pair – NEOSSat Recovery

Stuart Eagleson
Magellan Aerospace, Winnipeg
3701 Carling Avenue, Ottawa, ON, K2H 8S2, Canada; 613-820-1287
stuart.eagleson@magellan.aero

Viqar Abbasi, Natasha Jackson
Canadian Space Agency
6767 Route de l'Aéroport, Saint-Hubert, PQ, J3Y 8Y9, Canada; 450-926-5844
viquar.abbasi@canada.ca

Robert (Lauchie) Scott, Stefan Thorsteinson
Defence Research and Development Canada
3701 Carling Avenue, Ottawa, ON, K2H 8S2, Canada; 613-998-6503
lauchie.scott@drdc-rddc.gc.ca

ABSTRACT

In flight, the Near Earth Object Surveillance Satellite (NEOSSat) lost use of its single-string magnetometer that was necessary to coarsely solve the attitude problem and seed the satellite's star tracker for fine attitude determination. Unable to determine attitude, satellite control was lost and an ad-hoc, in-flight, solution was needed to recover operations. Building on existing GPS literature, NEOSSat's GPS receiver was augmented, in software, to estimate the antenna's look direction, in an inertial frame of reference. Matched with the known (mounting) vector in the body frame, a vector pair was successfully created that replaced the one from the magnetometer. This paper describes the mission context, algorithms, calibration methods, software implementation, testing (ground and flight) and optimizations that enabled the on-orbit GPS receiver to become a successful attitude sensor. The results, RMS errors within 10 degrees without mitigation of multipath effects, are generally applicable to satellites that have even just one GPS receiver and antenna and represent an alternate or back-up means of contributing to coarse attitude determination.

INTRODUCTION

This paper describes the use of GPS Carrier to Noise-Density Ratio (C/N_0) measurements to assist with attitude determination for the Near Earth Object Surveillance Satellite (NEOSSat).
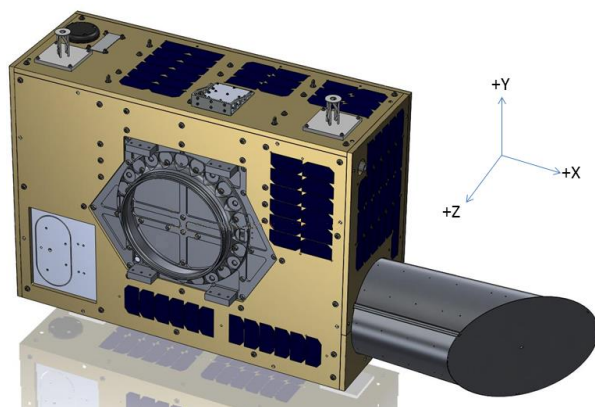

Figure 1: NEOSSat Rendering

Applying C/N_0 to the attitude-determination problem has been considered in the literature since the early days of the GPS constellation, but is not widely used in the design of attitude subsystems. Beyond uniquely applying the basic concept as an in-flight recovery method, some novel adaptations of existing literature were realized in the course of the NEOSSat recovery work that improve performance and are also described in this work.

Use of an Extended Kalman Filter (EKF) or other observer is now, but was not always, ubiquitous for on-orbit attitude determination. A consequence is that even coarse sensors can add useful information to a solution that includes fine sensors, with proper measurement weighting (Simon, 2006). Given that many nanosatellites and microsatellites now typically include a GPS receiver, an outcome of this work is the realization and exhortation that these receivers, for little work and positive benefit, can be used to augment attitude determination in-situ, either as part of nominal (coarse) sensing or as a back-up tool in cases of

primary-sensor failure. With some additional up-front design work to avoid obvious multipath issues, the potential is even greater.

NEOSSAT MISSION & SITUATION

NEOSSat is a 75 kg microsatellite, jointly funded by the Canadian Space Agency (CSA) and Defence Research & Development Canada (DRDC) and built by Microsat Systems Canada Inc. (MSCI), based on heritage of the MOST space telescope. Launched in February 2013 to an 800 km sun-synchronous low-Earth orbit, the satellite was designed for two distinct research missions on space situational awareness using a single 15 cm optical telescope: the Near-Earth Space Surveillance (NESS) mission, focused on near-Earth asteroids and the High-Earth Orbit Space Surveillance (HEOSS) mission, focused on tracking Resident Space Objects (RSO) in medium and high-Earth orbit. Overall mission objectives include demonstrating the utility and potential of relatively low-cost microsatellites as a platform for performing advanced tasks in space situational awareness and space astronomy.

The satellite's attitude determination and control system consists of a magnetometer and coarse sun sensor for three-axis coarse attitude determination, three rate sensors and a custom-built star tracker for fine attitude determination, which is collinear with the main telescope optics. Four momentum-biased wheels are used for pointing and slewing, while three torque rods are used for dumping excess momentum. Together, these units ensure accurate and stable pointing and tracking.

NEOSSat is also equipped with two GPS receivers, which were initially meant for precise orbit determination, not attitude determination. The receivers are not synchronized. Each receiver is connected to a single GPS antenna and the two antennas point in opposite directions – therefore precluding differential GPS techniques. The opposite-facing setup is designed to maximize viewing of the GPS constellation under different satellite attitudes, effectively operating with only a single GPS antenna-receiver pair.

As is common to satellites, NEOSSat is subject to a radiation environment that leads to occasional subsystem resets due to single-event upsets. In the spring of 2016, magnetometer performance became suddenly and permanently degraded, causing the loss of coarse attitude determination. NEOSSat's star tracker requires a sufficiently accurate coarse attitude estimate to be initialized. Without the coarse estimate, it became impossible for NEOSSat to perform any kind of attitude determination with its existing sensors and the satellite remained in a tumbling state.

Routine satellite communication was maintained and the operations team carefully monitored the tumbling satellite. When required, manual commands were issued to change wheel rates, in turn altering the tumble dynamics in order to maintain thermal safety and to ensure the spacecraft's batteries did not overheat. Meanwhile, a recovery team worked to find ways to resume operations in light of the lost magnetometer.

The first flight-software update (post incident) implemented a new satellite control mode, based solely on the coarse sun sensor, which enabled the satellite's orientation to be controlled with respect to the Sun. Although the missing degree of freedom meant that the satellite was free to rotate around the Sun vector, the new mode allowed thermal control of the vehicle without manual intervention, maintaining spacecraft health and safety while methods to recover attitude determination could be devised. In addition, the new Sun-pointing mode allowed operators to open the telescope shutter and take star images that could be processed offline to give attitude-truth data. The updated flight software also augmented the interface with the GPS receivers to capture advanced logs about GPS constellation Space Vehicles (SV) being tracked, including their position and signal-to-noise ratios. This additional information proved to be essential in creating a new GPS-based attitude sensor.

ALGORITHM

Axelrad and Wang are among those who have considered (Axelrad, 1999; Wang, 2003) the means of using a single GPS antenna to assist with attitude determination. The approach is illustrated by Figure 2, in which three GPS SVs are nadir-pointed. NEOSSat's antenna boresight $\mathbf{b}$ is arbitrarily pointed in an inertial frame of reference. This creates elevation-angle set α between the boresight and the sight lines to each SV. Measured C/N_0 has a primarily cosine relationship with α, locally maximized when $\mathbf{b}$ is pointed directly at an SV (global maximization occurs when the SV's receiver reciprocates direct pointing). The angular relationship is not a pure cosine due, in part, to idiosyncrasies of the inherent gain pattern and effects of mounting the antenna. Construction of a calibration map of α as a function of C/N_0 is therefore required. Azimuthal variations are typically small in the inherent gain pattern but can become pronounced in the presence of multipath effects.

The sight line to a given SV is known in the inertial frame but not in the body frame of reference. Angle α sweeps out a cone around the boresight and the sight line could lie anywhere on the cone, in the body frame. Adding in at least two other cones leads to a unique intersection of possibilities in the body frame. That is,
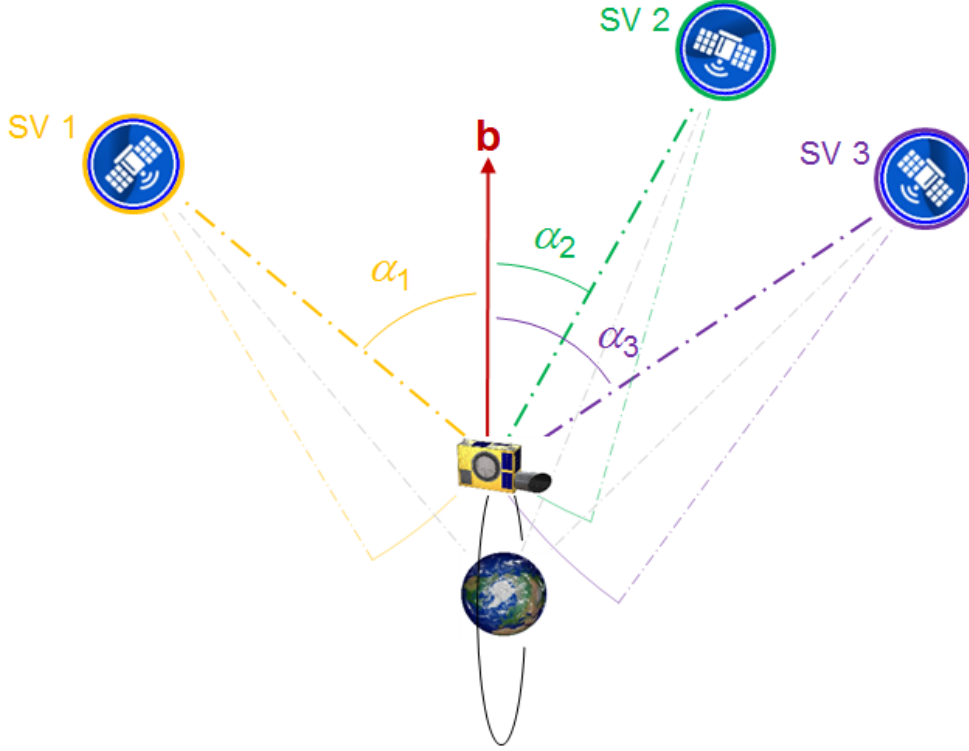
Figure 2: Lines of Sight and Angles

the mathematics of the problem centre on calculating the direction of **b** that best satisfies the measured elevation angles. Once determined, the calculated boresight in the inertial frame and the known boresight in the body frame (from satellite design and integration) form a vector pair that can be passed to an attitude observer.

$$J(\hat{\mathbf{b}}) = \frac{1}{2} \sum_{j=1}^{n} \frac{1}{\sigma_j^2} \left(\cos(\alpha_j) - \hat{\mathbf{b}}^{\mathrm{T}} \hat{\mathbf{s}}_j \right)^2 \qquad (1)$$

Equation 1 defines J, a cost function that solves for **b** in an inertial frame at a given instant in time. In this equation, $\mathbf{s}_j$ is the sight line from NEOSSat to SV j and σ is the level of uncertainty associated with the estimate of α (itself a function of C/N_0) for the same SV. Following the literature, the values of σ correspond to binned intervals of the calibration map, set to a size of 5 degrees for NEOSSat.

The cost equation sums over the range of $n \geq 3$ C/N_0 measurements that are available and valid at the given point in time. For NEOSSat, the sight lines are defined in an Earth Centered Earth Fixed (ECEF) frame of reference. ECEF vectors are provided by the receiver

for each tracked SV and are mapped into a J2000-based inertial frame and then corrected to the satellite's orbital position.

The solution of the cost function is typically iterative (Axelrad, 1999; Wang, 2003). For NEOSSat, a simplifying observation (Torresan, 2014) is applied, in which the solution is calculated in one step, using Equation 2.

$$\mathbf{b} = \mathbf{N}^{-1} \mathbf{z} \qquad (2a)$$

$$\mathbf{N} = \sum_{j=1}^{n} \frac{1}{\sigma_j^2} \hat{\mathbf{s}}_j \hat{\mathbf{s}}_j^{\mathrm{T}} \qquad (2b)$$

$$\mathbf{z} = \sum_{j=1}^{n} \frac{1}{\sigma_j^2} \cos(\alpha_j) \hat{\mathbf{s}}_j \qquad (2c)$$

In this equation, **N** is the summation of the weighted outer products of **s**, defined by Equation 2b, and **z** is the summation of the weighted projections of the sight lines onto the boresight, defined by Equation 2c. Once the estimate of **b** has been calculated, it is normalized before being passed to the attitude observer.

The typical use of iteration seeks an optimal solution and the use of only a single step means that the calculated vector is sub-optimal, to a degree not fully explored in this work. The measurement itself does not complete the attitude solution but is fed into an EKF, along with at least one other coarse vector pair (for NEOSSat, this corresponds to a Sun-vector pair). The EKF, itself a suboptimal filter, provides coarse attitude estimates. This approach saves the computational processing involved in an iterative solution, but is nonetheless able to achieve acceptable results and enabled successful satellite recovery.

Loss Compensation

Before C/N_0 measurements are used to estimate corresponding elevation angles, they are corrected to a common reference condition.

The carrier-to-noise-density ratio is a function of GPS SV transmit power P_{tx}, GPS SV transmit gain G_{tx}, NEOSSat's receiver gain G_{rx} and free-space path loss L_{fs}; Equation 3 defines the linear scale.

$$\frac{C}{N_0} = \frac{P_{tx}G_{tx}G_{rx}}{L_{fs}N_0} \qquad (3)$$

Considering P_{tx}, G_{rx} and N_0 to be equal for both the measured and reference conditions, C/N_0 corrected to arbitrary reference $C/N_0|_{ref}$ can be related to measured value $C/N_0|_{meas}$ as shown in Equation 4a, where d is separation distance.

$$\left(\frac{C}{N_0}\right)_{ref} = \left(\frac{C}{N_0}\right)_{meas} + \Delta G_{tx} + d^* \qquad (4a)$$

$$\Delta G_{tx} = G_{tx,ref} - G_{tx,meas} \qquad (4b)$$

$$d^* = 20\log\left(\frac{d_{meas}}{d_{ref}}\right) \qquad (4c)$$

Transmit gain correction has not yet been implemented for NEOSSat. C/N_0 measurements for NEOSSat have been made at up to 16 degrees off-boresight from a given SV's antenna. Based on publically available SV transmission characteristics (Marquis, 2015), these variations can yield a difference of up to 3 dB compared with measurements made in-line ($\theta = 0$). The transmit power of individual SVs can also vary by up to 0.7 dB. Despite the relatively substantial impact, gain correction in ground analyses did not substantially reduce the spread in the C/N_0-versus-elevation (α) map. One barrier to gain correction is a lack of publicly available data for the IIF block of GPS satellites. It is

possible that an improved calibration could be produced with analysis of extended observations from on-board data.

The correction, as applied to NEOSSat, is shown in Equation 5, with d_{ref} being arbitrarily set to 1 and ΔG_{tx} being excluded given the notes above.

$$\left(\frac{C}{N_0}\right)_{ref} = \left(\frac{C}{N_0}\right)_{meas} + 20\log\left(d_{meas}\right) \qquad (3)$$

Combined Mode

NEOSSat's two antennas have their boresights facing in opposite directions, along the satellite's Y axis. While precluding differential GPS techniques, this setup allows for an innovative improvement in the estimation of **b**. Consider Figure 3, where an SV is measured by receiver number 1 with a given angle estimated with respect to that antenna's boresight. Because antenna number 2 is mounted in the opposite direction, the Opposite Angle Theorem allows the sign of the sightline to be flipped while preserving the estimated elevation angle. Effectively, this means that SVs measured on one antenna can be combined into the set of measurements made by the other antenna. The main advantage of this simple-to-implement adaptation is that the cost function will solve over a greater number of SVs, generally improving accuracy (particularly when low numbers of SVs are involved).
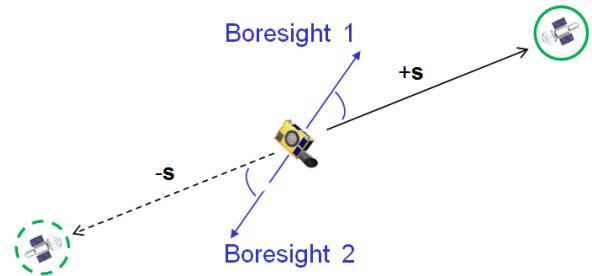
Figure 3: Flipping Sightlines

A second advantage of this combined mode is that it can minimize the impacts of multi-path effects and the host satellite's transparency to the received GPS signals. In practice, even though both GPS units are on opposite faces of the satellite, the two units often see a common subset of GPS SVs. The calibration map assumes that all visible SVs are "over the horizon" relative to the receiver and the presence of SVs being tracked below the horizon are simply a source of error in the algorithm. Left unchecked, the algorithms would

calculate two different sightlines in the body frame for the same SV, creating an ambiguity as to the correct angle in the body frame. This ambiguity is resolved in Combined mode by assuming that the SV with the smaller C/N0 is below the horizon relative to its receiver and therefore should be excluded. This means that if, for example, the +Y GPS receiver sees 6 SVs and the −Y GPS receiver also sees 6 SVs, two of which are also seen by the +Y GPS receiver, the total number of SVs used in the solution would be 10, not 12. Performance accuracy is improved when using 10 SVs with a higher degree of confidence to be above the horizon of the receiver, compared to using 6 or 12 where some below-the-horizon SVs are also included that would drive down the solution's accuracy.

Pseudo SVs

Equation 1 operates on elevation angle α; C/N0 is a stepping stone to finding the inner angle between an SV's sight line and the antenna boresight. This leads to the observation that the cost function can be augmented by other, non-SV, sight lines with the goal of improving performance. The Sun is one example: its sight line in an inertial frame is knowable using a solar ephemeris, which is commonly part of a satellite's attitude-determination software. The Sun's direction in the body frame is also commonly available on satellites, provided by Sun sensors. The angle between the Sun vector in the body frame and the antenna's boresight is therefore an elevation angle that can be calculated and included in the cost function.

Figure 4 illustrates a NEOSSat example, showing a polar graph centered on the antenna boresight's true direction (looking into the page), in an inertial frame. A number of SVs are being tracked, with red circles identifying calculated elevation angles and green, true elevation angles. The estimate of **b** is marked by a blue star. There is a notable spread of errors in α calculations, illustrated by the differing line lengths between calculated and true elevations. This spread is typical of NEOSSat's calibration map. By comparison, even coarse Sun sensors subjected to albedo can consistently offer at least a moderately accurate elevation angle that can be separately weighted in the cost function and positively contribute to the estimate. In the figure, the Sun's true location is marked by a yellow circle and (for this particular measurement) its estimate has an error of 3 degrees.

An added minor benefit to using the Sun or other pseudo-SV is that it reduces the number of true SVs that need to be tracked for the cost function to be solvable. That is, if only two SVs are tracked but the Sun is included, then the minimum requirement of three angles is achieved.
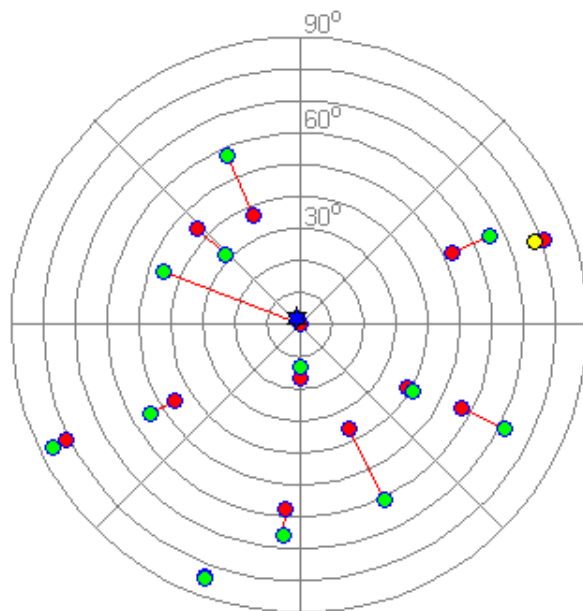
Figure 4: Antenna Polar Graph with Sun

While NEOSSat does not currently employ this novelty on-orbit as part of its flight software, post-processed application to flight telemetry shows improvements in the RMS error of about 2 degrees. Augmentation could similarly be made using a magnetometer (no longer available to NEOSSat) or any known vector in the body frame that has a corresponding model in an inertial frame of reference.

FLATSAT TESTING

Setup and Testing

All flight software updates are first tested on the NEOSSat flatsat, which includes a flight-spare main processor board with table-top connections to a subset of flight-like sensors and actuators, including one flight-like GPS receiver that is able to receive GPS signals repeated from a GPS antenna mounted on the roof of CSA's St-Hubert facility. This infrastructure proved to be valuable in support of developing and calibrating the new GPS attitude-sensor algorithm.

The new flight software, featuring augmented GPS logs, was executed over long periods of time, collecting and reporting in telemetry the position and signal-to-noise information for various GPS SVs passing overhead. This telemetry was post-processed and compared with ground knowledge of roof-mounted antenna's orientation to evaluate and improve performance of the GPS attitude sensor algorithm.

Results

Figure 5 shows about an hour's worth of flatsat telemetry parsed into a map of true elevation against measured C/N_0. A fourth-order polynomial fit is also shown. The horizontal spread is relatively low at low elevation angles (close to the antenna's zenith) and higher near the horizon. The reason for this is thought to (partly) be the fact that symmetry in azimuth is not as good on ground as on orbit because losses through the atmosphere (not a factor on orbit) differ over time and direction. Minor multipath effects could also be partially responsible. Overall, the calibration map allows a confident fit of the data to be applied.
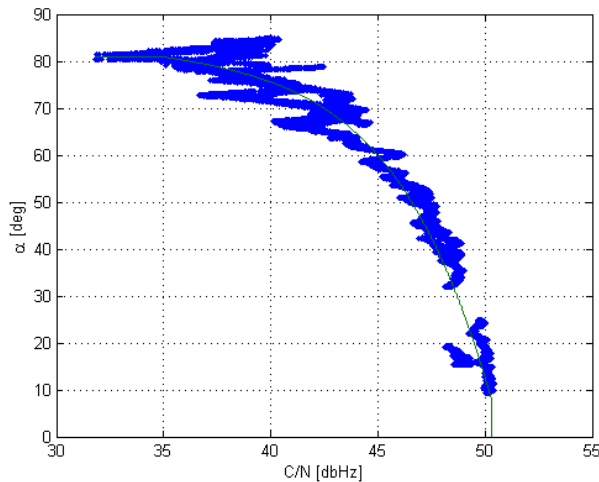
Figure 5: Flatsat Calibration Map

Figure 6 shows early flatsat results that have an RMS error of 3.1 degrees for estimation of **b** in an inertial frame of reference. The flatsat errors vary as a function of the number of SVs in view and their elevation angle. As long as most of the tracked SVs are 30 degrees or more above the horizon (below which the calibration map loses quality), the RMS errors are within a few degrees. Otherwise, the RMS errors can reach 10 degrees or (occasionally) more.
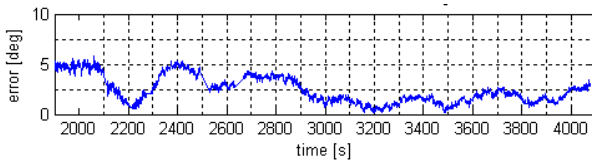
Figure 6: Flatsat RMS Errors

TRUE ATTITUDE

While the orientation of the flatsat GPS antenna is constant and well known, the same is not true about the orientation of the GPS antenna on the tumbling NEOSSat vehicle. For this flight case, a mechanism to determine the true attitude of the satellite is needed in order to develop and validate a flight calibration map for the satellite.

To construct a map that relates measured C/N_0 to an elevation angle requires knowledge of the antenna's true attitude. NEOSSat generated two main calibration maps: one based on ground tests and one based on flight telemetry. In all cases, raw C/N_0 measurements are loss-compensated prior to use.

Truth on Ground

Ground-based testing used NEOSSat's flatsat, an electrical equivalent to the satellite located at the CSA's headquarters. This configuration includes a flight-equivalent computer to evaluate flight-software updates as well as a flight-like GPS receiver connected to a roof-mounted GPS antenna. The flatsat GPS antenna is well-aligned with zenith and so the antenna's true attitude is the receiver's position estimate, expressed in an inertial frame rather than the receiver's native Earth-fixed frame. Knowledge of rotation around this direction is not necessary.

Truth on Orbit

On orbit, knowledge of the antenna's true attitude is much more challenging. Ideally, the star tracker would be used but is only available when coarse knowledge of attitude of about 4 degrees is achieved – which was not the case for NEOSSat after loss of its magnetometer. Instead, due to NEOSSat's loss of attitude knowledge, a multi-step process was devised to determine true attitude based on its main telescope.

To help ensure NEOSSat's survival, NEOSSat was placed into an approximately 4 degree/second spin about the Sun line, illuminating the satellite's -Z solar panel. This kept NEOSSat thermally stable, positively powered and safe to open the telescope's Sun-safety shutter. In order to obtain star imagery to determine true orientation, the spin needed to be temporarily arrested so that stars could be detected by its main telescope. A specialized Sun-pointing mode of attitude control was devised whereby NEOSSat can perform yaw and pitch corrections about the Sun line, but is free to roll about it. This new attitude control mode enabled NEOSSat to temporarily transfer its angular momentum into its reaction wheels, reducing the spin rate to less than 0.1 degrees/second. In this quasi-inertial Sun-point mode, star imaging is possible.

NEOSSat's telescope then acquires a series of short-exposure rapid-succession images to capture short streaklets of background stars. An example is shown on

the right side of Figure 7; the vertical line in each sub-image is a burned pixel column on NEOSSat's detector. As NEOSSat does not have roll control about the Sun line in this control mode, the Earth periodically blocks the telescope from the background stars. To mitigate this occultation, star imaging attempts occur over an entire orbit to increase the likelihood of detecting background stars while in Sun-point mode.
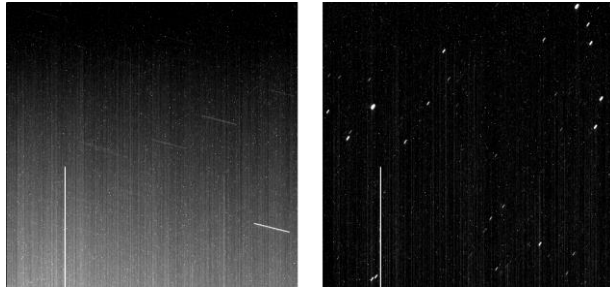
Figure 7: Raw Telescope Imagery

Image processing is challenging as the spinning attitude increases the temperature of the telescope's CCD from 0 to 10 degrees Celsius. This high CCD operating temperature causes imagery to be very noisy due to high dark current generation (see left side of Figure 7). Despite the high noise level of the imagery even under low-to-arrested spin (see right side of Figure 7), bright background star steaks can be successfully centroided and star positions are registered using the UCAC 3 star catalog. Each image-based star-solution enables arcsecond-accurate determination of pitch and yaw orientation and a few arc minutes of precision about the telescope's boresight. The resulting attitude data is considered accurate enough to be "truth" data for recovery purposes and was successfully used as such, principally by mapping the known body-fixed orientation of the GPS antenna into a standard inertial reference frame.

Simultaneously during star imaging, NEOSSat's GPS receiver is queried for detected GPS SV IDs, locations in an inertial frame, C/N_0 values and time of measurement. The image-based truth data can then determine the elevation of each tracked SV with respect to the inertial-referenced antenna boresight. Comparing these elevation angles with the measured C/N_0 values permitted creation of the first flight-derived calibration map – which had previously been based on flatsat results.

FLIGHT RESULTS

Once Sun-pointing control was available in flight software to allow ground-estimation of true attitude, a series of specific experiments were run to revise the calibration map and attempt to achieve attitude

knowledge sufficient to re-engage the star tracker. Each experiment involved inertial stabilization of NEOSSat, collecting flight telemetry and observing whether or not the net EKF attitude solution achieved the necessary accuracy. For each iteration between experiments, flight telemetry was used to estimate true attitude (ground-processed as described earlier) and revise the calibration map and its polynomial fit. Flight telemetry was also used to modify algorithm settings and EKF settings to improve performance. Eventually, sufficient accuracy was achieved and NEOSSat is now able to consistently use its star tracker and engage fine-pointing control.

Figure 8 shows typical flight results, where the RMS error in estimating **b** is 5.5 deg. RMS errors, over multiple data sets, span 0 to 10 degrees. At the far right of the figure, one can observe some dithering as the number of SVs used in solution drops and some toggle in-and-out of use.
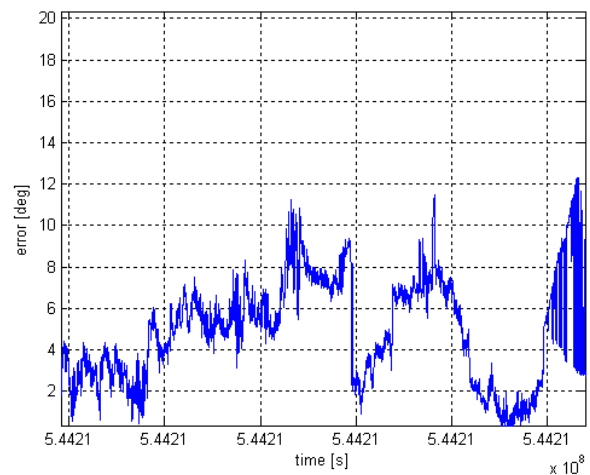
Figure 8: Flight RMS Errors

Figure 9 shows the corresponding number of SVs being tracked by the receiver, as well as the number of how many of the tracked SVs are being used by the GPS cost function.

For NEOSSat, there is a number of reasons that notably less SVs are used in boresight estimation than are tracked by the receiver. Primarily, the satellite appears quite transparent to the GPS L1 frequency and is able to pick up a number of SVs that are *below* the antenna's horizon, which are subsequently rejected in the GPS-boresight's combined-mode algorithm. Other reasons relate to the receiver's quality flags: tracking state, phase lock, parity, code lock and time lock.
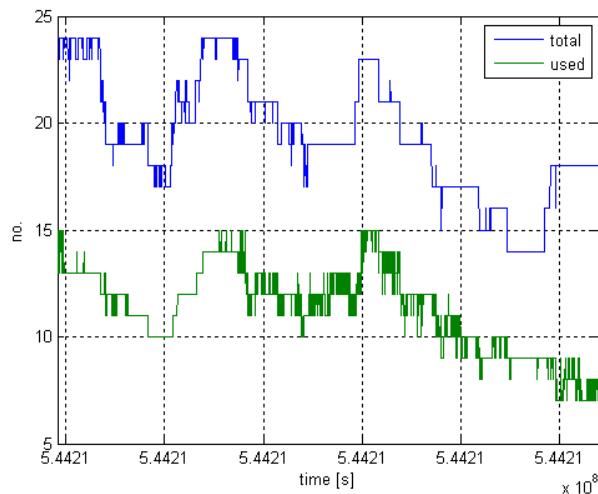
Figure 9: SVs Tracked and Used

Revised Calibration

Using the techniques described earlier to estimate true satellite attitudes on orbit, a revised calibration map was created, shown in Figure 10.
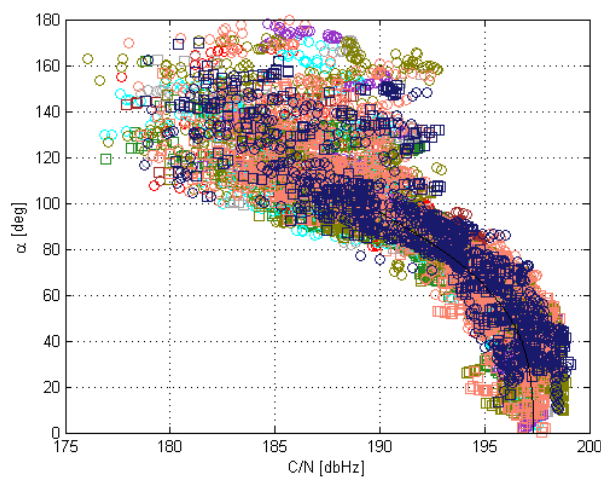
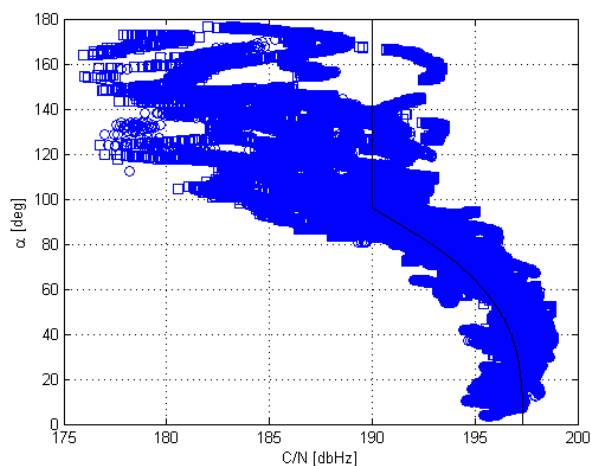
Figure 10: Flight Calibration Map

In this map, a number of data sets is overlaid, each marked by its own shape and colour and clearly consistent with each other. In comparing the results with the initial flatsat-based map, the overall trend above the antenna's horizon is quite similar but there is significantly more deviation around the polynomial fit. Multipath effects are suspected to be the prime cause of the increased measurement spread seen in flight, noting that the GPS antennas in both the +Y and -Y axes are located close to protruding objects.

The flatsat map used a traditional approach to loss-compensation (Axelrad, 1999), which does not account for full free-space losses, while the flight map uses the presented (and more complete) expression for loss compensation. The flight calibration map is also free of atmospheric losses.

Another interesting observation of the flight map is the density of measurements received from below horizon. NEOSSat turns out to be quite transparent to RF at the GPS L1 frequency and frequently tracks SVs at elevation angles above 90 degrees. However, the gain pattern below horizon is anisotropic and not useful for consideration in the cost function. In flight software, detected SV measurements below horizon are rejected.

After implementation of the GPS vector-pair algorithm enabled the star tracker to be used again, a third calibration map was created using star tracker measurements as the source of attitude truth rather than the ground-processed solutions. One of the benefits of using the star tracker for calibration is the density of measurements at 1 Hz. Figure 11 presents an initial construction of this map. Comparing to Figure 10, there is a high degree of similarity. An interesting arc-back appears at low elevation that has not yet been fully understood.

Figure 11: Star Tracker Based Calibration Map

Resumption of Operations

Initial GPS attitude-vector algorithms were uploaded to NEOSSat in the second half of 2016. Flight telemetry was then analyzed and algorithms tweaked to improve performance. In March 2017, NEOSSat achieved fine pointing once again. At the time of writing, NEOSSat continues to support space surveillance activities for CSA and DRDC. Figure 12 shows an image of M20 taken by NEOSSat while fine pointing, post-recovery, in June 2017.
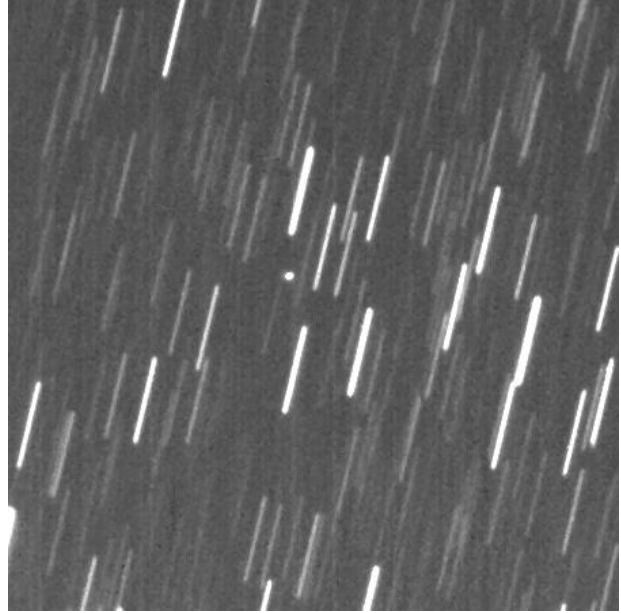
Figure 12: M20 (Trifid Nebula) by NEOSSat

Figure 13: 2012-TC04 by NEOSSat

With increasing confidence in restored attitude-control capabilities, NEOSSat contributed to the 2012-TC04 observation campaign (U. Maryland, 2017). This international campaign refined and practiced techniques of the asteroid-observation community to mitigate the risks of future Potentially Hazardous Asteroid (PHA) collision with the Earth, if such a risk were ever forecast. The campaign organizers selected the small, 10 m sized asteroid 2012-TC04 as a campaign practice target because it was predicted to pass 50 000 km from Earth on 12 October 2017, mimicking the encounter geometry of a real asteroid threat.

NEOSSat's contribution to this effort was to attempt observations of the asteroid during its pass onto Earth's day side. Ground-based telescopes are unable to detect the asteroid during its pass onto the day side as they cannot operate in daylight. NEOSSat, unaffected by the day-night cycle, can continue to collect measurements until the asteroid passes within 45 degree of the Sun.

On 11 October 2017, when 2012-TC04 entered inside lunar orbit and within NEOSSat's detection capabilities, the NEOSSat mission team dedicated two days of observations of the asteroid as it closed in on Earth.

Figure 13 shows an image of 2012-TC04 (central dot) taken by NEOSSat while the asteroid was passing Earth 53 000 km over the southern Pacific. The streaks in the figure are background stars used to measure the astrometric position of the asteroid.

Brightness measurements collected by NEOSSat on 2012-TC04 during are shown in Figure 14.
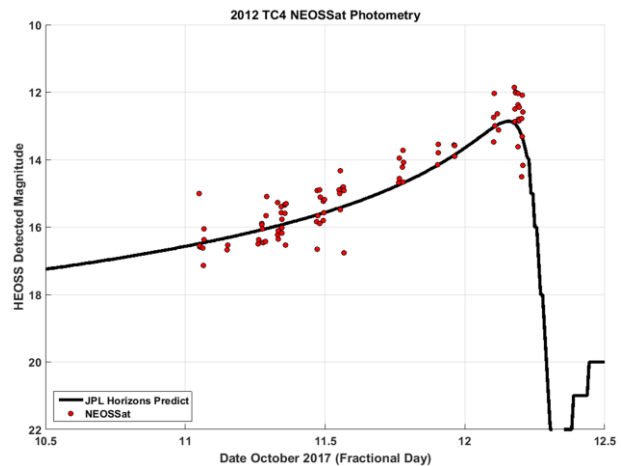
Figure 14: 2012-TC04 Photometric Curve

The 1.5 magnitudes of scatter in the light curve are due to the 12 minute rotational period of the asteroid causing its variation in brightness. Once the asteroid's path got too close to the Sun, NEOSSat's Sun safety shutter closed, completing the observation attempt. NEOSSat observations were aggregated with the other optical and radar observations collected by other observatories, completing Canada's contribution to the campaign.

CONCLUSION

NEOSSat presented a strong challenge to use available in-flight hardware as well as software modifications to

compensate for a lost magnetometer. Building on existing literature with a couple of novel adaptations resulted in NEOSSat's GPS receiver being augmented to serve as an attitude sensor. Estimating the antenna's boresight in the inertial frame of reference and knowing the boresight's direction in the body frame by design, the algorithm creates a vector pair that feeds into the satellite's EKF, replacing the vector pair that had previously been provided by the magnetometer. Even in the presence of multipath effects, RMS errors of the GPS attitude sensor are typically 10 degrees or better.

While there is some novelty in the work presented, the key aspiration of this paper is to affirm that single-antenna GPS receivers, common on nanosatellites and microsatellites, can serve a dual purpose and therefore contribute to attitude determination in a meaningful way. For little work and cost that is entirely software based, complementary or back-up attitude sensing is made possible for satellites already on orbit and could become more commonly employed in the field. As noted earlier, a little hardware design work up front, in the form of keeping GPS antennas clear from nearby protrusions and or adding choke rings, would notably help reduce multipath effects and improve performance results.

The main outcome and highlight of this work is that the NEOSSat mission, once jeopardized by unexpected unit failures – in the magnetometer and elsewhere as described by Abbasi [7], has been successfully recovered and continues to operate well.

ACKNOWLEDGMENTS

REFERENCES

1. Simon, D., Optimal State Estimation, John Wiley & Sons, 2006.

2. Axelrad, P. and Behre, C., "Satellite Attitude Determination Based on GPS Signal-to-Noise Ratio", Proceedings of the IEEE, vol. 87, no. 1, 1999.

3. Wang, C., "Single-antenna attitude determination for Fedsat with improved antenna gain patterns", Proceedings of the 6th International Symposium on Satellite Navigation Technology, paper 25, 2003.

4. Torresan, S., Development and Analysis of a New DGPS Attitude Determination Method for Miniature Satellites, Padova University, 2014.

5. Marquis, W., "The GPS Block IIR/IIR-M Antenna Panel Pattern", Lockheed Martin Corp., 2015.

6. University of Maryland, "The 2012 TC4 Observing Campaign", http://2012tc4.astro.umd.edu, 2017.

7. Abbasi, V., "NEOSSat Recovery Following Magnetometer and Torque Rod Failure", Proceedings of the AIAA SpaceOps conference, 2018.